Supramolecular Assemblies of a Semirigid Polyanion in Aqueous Solutions

ARTICLE *in* MACROMOLECULES · APRIL 2013

Impact Factor: 5.8 · DOI: 10.1021/ma400428n

Macromolecules

Article

pubs.acs.org/Macromolecules

Supramolecular Assemblies of a Semirigid Polyanion in Aqueous Solutions

Zi Liang Wu,[†] Md. Arifuzzaman,[†] Takayuki Kurokawa,[‡] Khoa Le,[‡] Jian Hu,[†] Tao Lin Sun,[†] Hidemitsu Furukawa,[‡,∥] Hiroyasu Masunaga,[§] and Jian Ping Gong*[,‡]

[†]Division of Biological Sciences, Graduate School of Science, Hokkaido University, Sapporo 060-0810, Japan

[‡]Faculty of Advanced Life Science, Graduate School of Science, Hokkaido University, Sapporo 060-0810, Japan

[§]Japan Synchrotron Radiation Research Institute (JASRI/SPring-8), Sayo-gun, Hyogo 679-5198 Japan

ABSTRACT: In this article, we report the supramolecular assemblies of a semirigid polyelectrolyte, poly(2,2′-disulfonyl-4,4′-benzidine terephthalamide) (PBDT) in water. Cryo-TEM observation and SAXS measurement reveal that PBDT forms bundle-like structure even in very dilute concentration, C_P, of 0.02 wt %. These bundle-like assemblies serve as new primary building blocks and self-assemble further as C_P increases, to form large associations with or without long-range orientation. When 2 wt % < C_P < 6 wt %, liquid−liquid phase separation occurs. Some of the supramolecular associations form bipolar liquid crystalline (LC) droplets via a typical nucleation and growth process. The droplets grow up by the coalescence of small ones and sediment under the gravity and coalesce to form a bottom nematic phase. When $C_P \geq 6$ wt %, the solutions are in a uniform nematic phase. The existence of these preliminary supramolecular assemblies of PBDT in aqueous solutions should be crucial for the formation of nematic LC phase at a significantly low C_P, as well as the formation of macroscopic ordered structures in hydrogels via electrostatic interaction between PBDT and oppositely charge multivalent metallic ion or polycation.

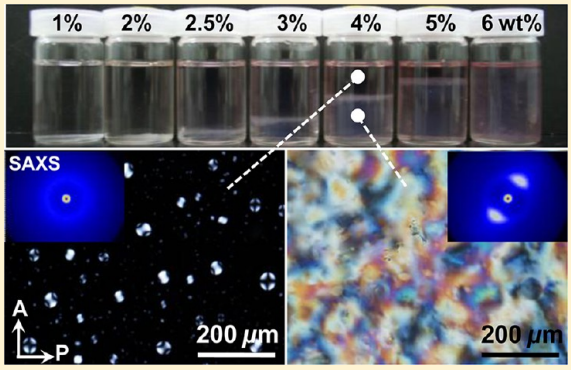

INTRODUCTION

Water-soluble rod-like macromolecules are ubiquitous in living organisms, such as deoxyribonucleic acid (DNA), microtubule (MT), and actin filaments (F-actin).[1−5] These biomacromolecules usually carry negative charges along with the rigid or semirigid structures, endowing them with great abilities to form advanced architectures, which are crucial for generating elaborate functions of living organisms.[5−11] For example, myosin shows a liquid crystalline (LC) structure in sarcomere, contributing to the formation and smooth motion of muscle fibers.[2] Safinya et al. have reported that DNA and cationic liposomes form complex and self-assemble into supramolecular LC phases (e.g., lamellar phase and inverted hexagonal columnar phase), which are supposed to be significant in gene delivery.[10,11] However, the essential structure formation mechanisms are usually hard to investigate *in vivo* because of the complex biomolecular structures and unstable biological environments. In the case of *in vitro* studies, the natural biomacromolecules with the secondary structure are difficult to tune without denaturation during the extraction and chemical reaction. In alternative, it is feasible and significant to study the self-assembling behaviors of synthetic semirigid polyelectrolytes that mimic the natural biomacromolecules.[12−19]

Wegner et al. have found that a rigid polyelectrolyte, dodecyl-substituted poly(*p*-phenylene)sulfonate (PPPS), forms cylindrical micelles in dilute aqueous solutions, even at a concentration as low as 0.001 g/L.[12−15] These micelles undergo further interactions at high polymer concentrations and form high ordered structures via axial or side-by-side aggregation. Mendes et al. have synthesized a series of sulfonated polyimides such as poly(*p*-sulfophenylene-terephthalamide) (sulfo-PPTA). The aqueous solutions of these polymers show uniform nematic LC phases at a significant low polymer concentration, around 2 wt %.[16−19] They ascribed this ordered structure formation at such low concentration to the presence of supramolecular assemblies that behavior as the building blocks of the nematic phase. In recent years, we focused on the self-assembly behaviors of a synthetic semirigid polyanion, poly(2,2′-disulfonyl-4,4′-benzidine terephthalamide) (PBDT), in the aqueous solutions and hydrogels.[20−32] The chemical structure of PBDT is shown in Scheme 1. We found that (i) PBDT aqueous solutions also show a significantly low critical concentration of nematic phase, C_{LC}*, of 2.8, 2.2, and 1.5 wt % for weight-average molecular weight, M_w, of 8×10^4, 1.8×10^6, and 2.6×10^6, respectively, much lower than those of common lyotropic LC macromolecules;[33] (ii) PBDT forms a variety of the self-assembling structures in aqueous solutions, ranging from isotropic cluster associations to fiber-like anisotropic

Received: February 27, 2013
Revised: April 9, 2013
Published: April 18, 2013

   dx.doi.org/10.1021/ma400428n | *Macromolecules* 2013, 46, 3581−3586

Scheme 1. Chemical Structure of PBDT

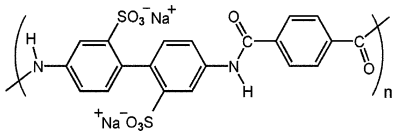

assemblies;[21] (iii) structured gels have been developed by the polymerization of the isotropic solution of a cationic monomer in the presence of PBDT as dopant[22−28] or by diffusion of Ca^{2+} into PBDT solution.[29−32]

In our previous work, we postulated that the significantly low C_{LC}* of PBDT solutions and the versatile self-assembling behaviors are closely associated with the semirigid structure and high M_w of PBDT.[20,21] However, the effect of M_w of PBDT on C_{LC}* does not follow Flory's lattice theory,[34,35] i.e. $C_{LC}^* \sim 8/X \sim 8/N \sim 8/M_w$, where X and N are the axial ratio and polymerization degree of the macromolecule, respectively. Because PBDT has a quite similar chemical structure to sulfo-PPTA that was studied by Mendes et al.,[16] we expect that the significantly low C_{LC}* of PBDT solutions and the capacity to form macroscopic anisotropic structures of PBDT in hydrogels are also owing to the existence of supramolecular assemblies even at very dilute concentration. These supramolecular assemblies are stable and serve as building block for the further self-assembly. To confirm this hypothesis, we study further the self-assembling behaviors of PBDT in aqueous solution with M_w of 1.8×10^6 and C_{LC}* of 2.2 wt %.

Here, we report the extraordinary supramolecular assemblies of PBDT formed in the aqueous solutions. Small angel X-ray scattering (SAXS) and transmission electron microscopy (TEM) results demonstrate the existence of bundle-like supramolecular assemblies even in the optically isotropic solution with C_P of 0.02 wt %. As C_P increases, PBDT solutions transfer from isotropic state with randomly dispersed bundle-like supramolecular assemblies, to biphasic phase of LC droplets (termed tactoids) dispersed in isotropic solution, and finally to a uniform nematic LC phase. After long time storage, the solutions with 2 wt % < C_P < 6 wt % separate into two aqueous phases. The upper transparent solution is an isotropic phase with dispersed dipolar LC droplets, and the bottom translucent one is a nematic phase.

EXPERIMENTAL SECTION

PBDT Synthesis. PBDT was prepared by an interfacial polycondensation reaction, as described elsewhere.[36,37] Gel permeation chromatography (GPC) was performed with a HITACHI L-7110 pump and a HITACHI 7490 RI detector using a SHODEX OHpak SB-805HQ column and 0.5 M CH_3COOH + 0.2 M $NaNO_3$ as the elution solvent. Poly(sodium *p*-styrenesulfonate) (PNaSS) was used to establish a standard curve. The weight-average molecular weight, M_w, and polydispersity (M_w/M_n) of PBDT were 1.8×10^6 and 1.2, respectively.

Phase Separation Measurement. PBDT aqueous solutions were prepared by dissolving a prescribed amount of PBDT in pure water. These solutions were stored without shaking for 2 months to achieve the stable state. The two separated phases were collected by a pipet and preserved in different bottles for the following characterizations. The PBDT concentration after phase separation was determined by measuring the absorbance at 302 nm using a UV−vis spectrophotometer (Hitachi U-3000). Serials of prescribed solutions with different C_P were used to make the standard curve. Then the absorbance of phase-separated solutions diluted 100 times was measured. The concentrations were calculated according to the standard curve.

Polarizing Optical Microscope (POM) Observation. Aqueous solutions were sandwiched between two glass plates and observed at room temperature under a POM (Nikon, LV100POL) with 530 nm sensitive tint plate (termed as full-wave plate or lambda (λ) plate). Shearing induced birefringence of PBDT aqueous solution was observed to establish the relationship between the molecular orientation and birefringence color. A 2 wt % PBDT aqueous solution was dripped onto a slide glass which was then covered by another one. The spacing between the two slide glasses was kept at 500 μm. The specimen was observed under POM while shearing was applied by translational or circular motion of the upper slide glass. To observe the change of assembled state under the evaporation process, one drop (~25 μL) 1 wt % PBDT solution was dripped on a slide glass by a pipet to form a thin liquid film. The morphologic evolution was observed at room temperature under the POM.

Small Angle X-ray Scattering (SAXS) Measurement. PBDT aqueous solutions were put into a cell consisting two parallel kapton films with 1 mm spacing. SAXS measurements were carried out at the BL40B2 of SPring-8, Japan Synchrotron Radiation Research Institute, using an incident X-ray with the wavelength of 0.16 nm. Scattered X-rays were detected by using an imaging plate with a resolution of 0.1 mm/pixel and keeping 3250 mm of sample-to-detector distance.

Transmission Electron Microscopy (TEM) and Cryo-TEM Observations. Samples fixed on carbon-coated copper grid were characterized by TEM or cryo-TEM (Hitachi H-7605). For TEM observation, additional staining was employed to increase the image contrast. A 10 μL PBDT solution was dripped onto the grid and left for 3 min. Most of the water was removed by using a filter paper wedge to touch the grid edge. Then, 10 μL of uranyl acetate solution (2 wt %) was dripped on the grid immediately and left for 1 min. The excess stain was removed by blotting with a filter paper wedge, and the sample was allowed to dry at room temperature.

Cryo-TEM vitrified samples were prepared using a custom-built chamber of controlled environment vitrification system (CEVS). All the samples were prepared at room temperature. In the CEVS, 5 μL of PBDT solution was dripped on a cryo-TEM grid, which was then soaked by a filter paper, resulting in the formation of thin liquid films of 10−300 nm. After a minimum 30 s detainment, the sample grid assembly was rapidly dipped into the liquid ethane at its melting point. The vitreous specimen was stored under liquid nitrogen until it was transferred to a cryogenic sample holder (Gatan 626).

RESULTS AND DISCUSSION

Since the semirigid PBDT is a lyotropic liquid crystalline polymer (LCP), its aqueous solutions show shear-induced birefringence due to the isotropic−nematic transition.[20,38] In our case, we use PBDT solution with C_P = 2 wt % < C_{LC}* = 2.2 wt %, which is optically isotropic. However, it shows strong birefringence (i.e., first-order gray-white color) observed under POM when a translation or circular shear is applied, resulting in the semirigid PBDT molecules to orient along with the shear direction (Figure 1). With insertion of 530 nm tint plate (λ-plate), different orientations of PBDT exhibit different birefringent colors due to addictive or subtractive effect of the specimen and λ-plate. When PBDT orients in a northwest−southeast direction, subtractive orange birefringence appears (Figure 1, right column), indicating that PBDT is a positive LCP.[38] Thus, we establish a direct relationship between the birefringent color and PBDT oriented direction, providing a visualized method to characterize the ordered structures formed in aqueous solutions and hydrogels.[27,30,31]

The solid PBDT quickly dissolves in water to form homogeneous solution for the first several days. However, the aqueous solutions in a certain range of C_P are metastable, and phase separation occurs after long time storage of the samples. As shown in Figure 2a, the PBDT solutions with 2 wt % < C_P < 6 wt % separate into two phases after two months storage at

dx.doi.org/10.1021/ma400428n | Macromolecules 2013, 46, 3581−3586

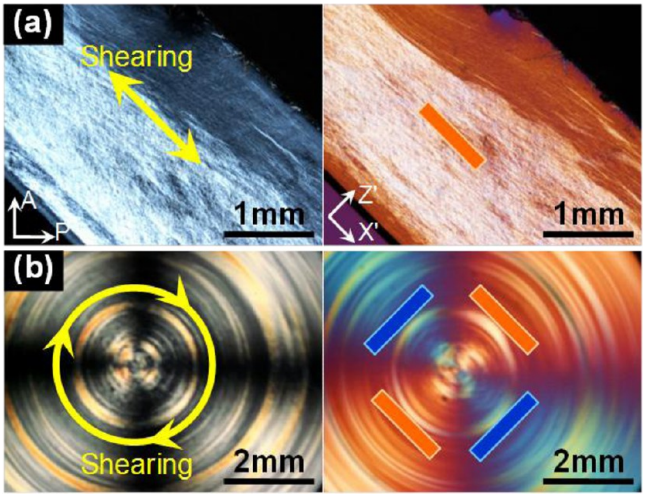

Figure 1. Micrographs of 2 wt % PBDT aqueous solution under translation shearing (a) and circular shearing (b) observed with crossed polarizers without (left column) and with (right column) λ-plate. A: Analyzer. P: Polarizer. X': Fast axis of the λ-plate. Z': Slow axis of the λ-plate.

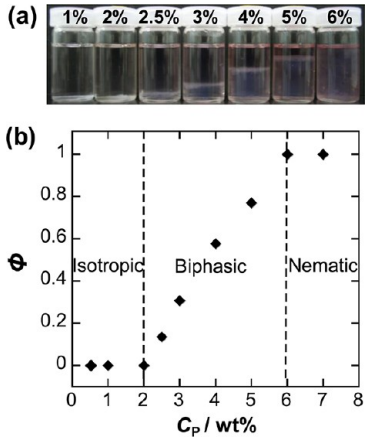

Figure 2. (a) Appearance of PBDT aqueous solutions with different concentrations after two months storage at room temperature. (b) Volume fraction, Φ, of the nematic phase as a function of total PBDT concentration, C_P.

room temperature. The volume fraction of the bottom nematic phase, Φ, increases linearly with C_P (Figure 2b).[39] C_P of the bottom phase is slightly higher than that of the upper phase. For example, the original 3 wt % PBDT solution separates into the upper and bottom solutions with C_P of 2.9 and 3.1 wt %, respectively. Similar phase separation phenomena are reported for other lyotropic LCP systems.[17,40,41]

The upper phase is transparent and includes many dispersed LC colloids with the diameter up to several tens of micrometers, showing clear Maltese crosses under POM (Figure 3, parts a and b). From the birefringent colors observed with λ-plate, we can confirm that PBDTs form a bipolar structure in these colloids (Figure 3c).[42−44] In addition, these LC droplets have a slightly elongated nonspherical shape, owing to the balance between surface tension and anisotropic elasticity, in which the former one favors a spherical surface, yet the latter one favors a cylindrical uniaxial surface. The lower phase shows a colorful schlieren texture that is the characteristic of nematic phase (Figure 3d). When $C_P \leq 2$ wt %, the solutions

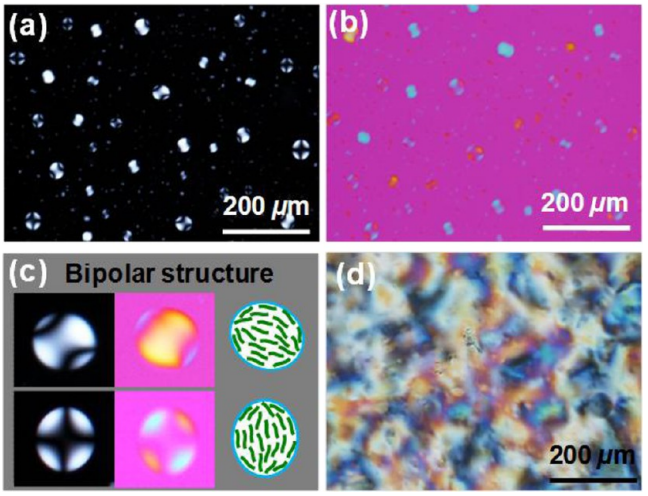

Figure 3. (a, b) POM images of the upper phase of 4 wt % PBDT solution after phase separation observed under crossed polarizers without (a) and with λ-plate (b). (c) Micrographs of single LC droplet with bipolar structure as shown in the scheme. (d) POM image of the bottom phase of 4 wt % PBDT solution after phase separation observed under crossed polarizers.

are optically isotropic and no dispersed colloids could be observed under POM. On the other hand, the solutions are in a uniform nematic phase, when $C_P \geq 6$ wt %.

SAXS measurements are performed to characterize the different assembled structures of PBDTs at nanometer scale. Isotropic scattering pattern is observed for the isotropic concentration region ($C_P \leq 2$ wt %). In the biphasic concentration region (2 wt % < C_P < 6 wt %), similar isotropic scattering pattern is observed for the upper transparent phase (Figure 4, inset A). On the other hand, an additional strong

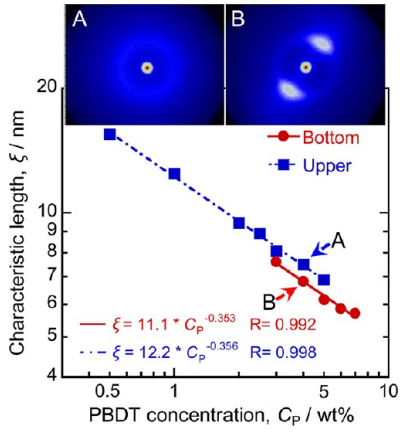

Figure 4. SAXS characteristic lengths of PBDT aqueous solutions, ξ, against the total PBDT concentration, C_P. Insets are the scattering patterns of the upper (A) and bottom (B) solutions of 4 wt % solution after phase separation.

anisotropic scattering pattern, superimposed on the isotropic one, is observed for the bottom nematic phase (Figure 4, inset B). Similar anisotropic scattering pattern was also observed for the nematic solutions with $C_P \geq 6$ wt %.

The characteristic length ξ, estimated from the maximum scattering vectors q_m using the relation $\xi = 2\pi/q_m$, is shown in Figure 4. The ξ observed from the isotropic or anisotropic scattering, decreases with the increase in C_P, showing a scaling

dx.doi.org/10.1021/ma400428n | Macromolecules 2013, 46, 3581−3586

relation of $\xi \sim C_P^{-1/3}$ (or $q_m \sim C_P^{1/3}$), regardless of the concentration regions defined in Figure 2. These results indicate that ξ observed for the upper biphasic phase with 2 wt % < C_P < 6 wt % is not from the dispersed LC colloids but from the background solution, because the isotropic solutions with $C_P \leq 2$ wt % that does not have dispersed colloids also showed a similar scattering pattern and a common scaling law of $\xi \sim C_P^{-1/3}$. Furthermore, when 2 wt % < C_P < 6 wt %, ξ of bottom nematic phase is slightly smaller than that of the upper isotropic phase.

A scaling relationship $q_m \sim C_P^{1/3}$ is usually found in dilute solution of biopolymers with local rigid structure; for semidilute solution, $q_m \sim C_P^{1/2}$.[45−47] For a flexible polymer of equivalent molecular weight $M_w = 1.8 \times 10^6$, the solutions with C_P up to 7 wt % is in the semidilute or concentrated region, yet in our case they still follow the relationship $q_m \sim C_P^{1/3}$.

We speculate that PBDTs form supramolecular assemblies even in the very dilute solution, which behavior as new units and therefore greatly decrease the concentration of assemblies.[16,48] The characteristic length ξ should be associated with the distance between aggregates.[16]

The existence of supramolecular assemblies at very dilute solution is confirmed by cryo-TEM observations of both 0.02 and 0.1 wt % PBDT solutions (Figure 5, parts a and b). Each

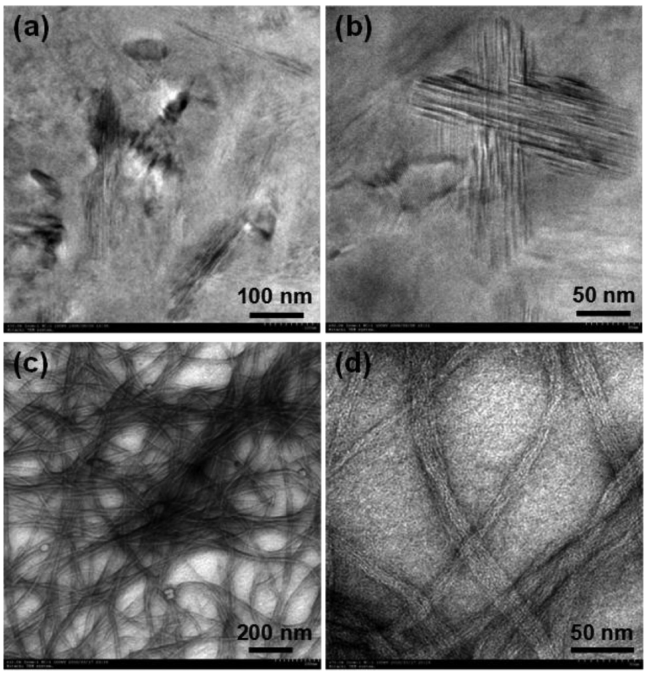

Figure 5. (a, b) Cryo-TEM images of 0.02 wt % (a) and 0.1 wt % (b) PBDT solutions. (c, d) TEM images of 0.5 wt % PBDT solution.

assembly consists of tens of PBDTs that align parallel to form an anisotropic bundle; the bundle-like assemblies are randomly dispersed without long-range orientation in the solutions. The intermolecular spacing, d, is ∼2 nm, much smaller than ξ determined by SAXS. As C_P increases, these preliminary supramolecular assemblies, as the building block, self-assemble further to form larger associations with or without long rang orientation.[49] As shown in Figure 5, parts c and d, an isotropic fibrous structure is formed in the solution with C_P = 0.5 wt %. It is noticed that the diameter of the fibers in TEM image is smaller than that observed by cryo-TEM, probably because the structure becomes more compact during the solvent evaporation process when the sample is prepared. We cannot observe these oriented structures of solution in nematic phase by TEM, because the dry samples on the copper grid prepared from PBDT solution with $M_w = 1.8 \times 10^6$ and C_P > 2 wt % are too thick to obtain a clear TEM image. However, we have observed the oriented fibers in low M_w PBDT solution ($M_w = 8 \times 10^4$, C_P = 4 wt %).[20]

PBDT molecules with super high M_w prefer to form bundle-like supramolecular assemblies even in very dilute solutions. The good solubility of a common polyelectrolyte is entropy-driven; the dissociation of counterions greatly increases the entropy of the system. For the PBDT system, this effect might be overwhelmed by the strong hydrophobic interaction, especially the strong $\pi-\pi$ packing between the main chains. If we consider the effect of hydration, this interaction might also be entropy-driven. Water molecules surrounding the hydrophobic main chains form ice-like structures to avoid the interaction with the main chains, and thus in low entropy state. When the hydrophobic molecules aggregate, these water molecules can be released back to the free state, thus the system gains high entropy.[50] The existence of these preliminary supramolecular assemblies should be crucial for the formation of nematic LC phase at a significantly low C_P. The local C_P inside the assembled domains should be much higher than that of the background solution, corresponding to a relatively high anisotropic refractive index. If the assemblies have long-range orientation, the solution will show strong birefringence at a significant low C_P.

To find the relationship between the different states of isotropic solution, biophasic phase with dispersed LC droplets, and uniform nematic phase, we directly observe the state transition during the solvent evaporation process of an isotropic solution.[51,52] One drop of 1 wt % PBDT solution is dripped onto a slide glass to form a thin solution film that is optically isotropic due to the relatively low C_P (Figure 6a). As the solvent evaporates at room temperature, the local C_P near the edge of the drop first increases, leading to the nucleation−growth phase separation to form LC droplets (region B in Figure 6b). These droplets with the size of several tens of micrometers exhibit Maltese cross under POM, indicating that PBDTs within the droplets orient into the bipolar structure (Figure 6c).[45,53] The small LC droplets coarsen further to grow in size (see the circled regions in Figure 6, parts e and f). The droplets are finally absorbed into the nearby uniform nematic phase; for example, the droplets showed by red arrows in Figure 6d are absorbed in the following process. This process will proceed forward to gradually change the isotropic solution to a nematic phase via a midcourse of nucleation and growth whereupon micrometer-sized LC droplets form.

On the basis of these results, we propose a mechanism for the transformation between different assembly states of PBDT in aqueous solutions with different C_P. PBDTs form preliminary supramolecular assemblies with anisotropic bundle structure that are randomly dispersed in the isotropic solutions. As C_P increases, these supramolecular assemblies, as the basic building block, self-assemble further to form large associations. When C_P > 2 wt %, some of the supramolecular associations form LC droplets with bipolar structure via a typical nucleation and growth process. The droplets grow up to ∼50 μm diameter by the coalescence of small ones. These relatively large droplets sediment under the gravity and coalesce to form a bottom nematic phase, where the long-range orientation plays

dx.doi.org/10.1021/ma400428n | Macromolecules 2013, 46, 3581−3586

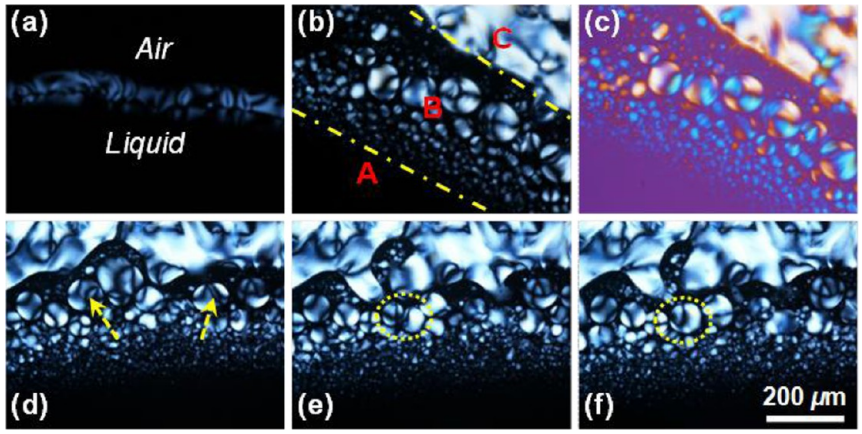

Figure 6. Morphologic evolution of 1 wt % PBDT solution film under solvent evaporation at room temperature. (a) At the initial state, the solution is optically isotropic. (b, c) As the solvent evaporates, C_P near the air−liquid interface increases, inducing the isotropic-to-nematic transition to form a nematic phase via a nucleation−growth process. The regions A, B, and C correspond to the isotropic phase, phase separation (nucleation−growth) phase, and nematic phase, respectively. (d−f) Small droplets coarsen (highlighted by the circles) to form large droplet that is further absorbed (highlighted by the arrows) into the uniform nematic phase. All the images are observed under polarizing microscope; image c is observed with the insertion of a λ-plate.

functions.[44,48] In the phase separation region, the upper transparent solution, which contains randomly dispersed PBDT bundle assemblies and LC droplets, and the bottom nematic phase as the reservoir, which consists of massive tactoids with long-range orientation by coarsening, are in a thermodynamic equilibrium state. This should be responsible for the linear increase of the nematic phase volume ratio with the increased C_P in Figure 2b. When C_P is above a critical value, the whole solution is in a uniform nematic phase.

■ CONCLUSIONS

In this paper, we have studied extraordinary assembling behaviors of a semirigid polyelectrolyte PBDT with a super high M_w in aqueous solutions. PBDTs in solutions with different C_P possess different aggregation states. When $C_P \leq 2$ wt %, primary bundle-like assemblies exist, which are randomly dispersed in the isotropic solutions even with C_P as low as 0.02 wt %, as directly observed by cryo-TEM. In the intermediate region, 2 wt % < C_P < 6 wt %, liquid−liquid phase separation occurs. The upper solutions are transparent and possess many LC colloids with dipolar structures; the bottom ones are translucent and in a nematic phase. When C_P > 6 wt %, the solutions become a uniform nematic phase. The isotropic solution with dispersed LC droplets is a transition state between the randomly dispersed assemblies and the nematic phase, as observed during the solvent evaporation process of an isotropic solution. In addition, the existence of primary supramolecular assemblies even in the dilute solutions, which behavior as new building block to self-assemble further and form large associations, should be significant for the formation of nematic phase at a super low C_{LC}* of PBDT, as well as the formation of unique macroscopic ordered structures in hydrogels.

■ AUTHOR INFORMATION

Corresponding Author

*E-mail: (J.P.G.) gong@mail.sci.hokudai.ac.jp.

Present Address

[‖](H.F.) Department of Mechanical Systems Engineering, Graduate School of Science and Engineering, Yamagata University, 4-3-16 Jonan, Yonezawa-shi, Yamagata 992−8510, Japan.

Notes

The authors declare no competing financial interest.

■ ACKNOWLEDGMENTS

This research was financially supported by a Grant-in-Aid for Scientific Research (S) (No. 124225006) from Japan Society for the Promotion of Science (JSPS).

■ REFERENCES

(1) Branden, C.; Tooze, J. *Introduction to Protein Structure*, 2nd ed.; Taylor & Francis: New York, 1999.
(2) Coppin, C. M.; Leavis, P. C. *Biophys. J.* **1992**, *63*, 794.
(3) Tang, J. X.; Janmey, P. A. *J. Biol. Chem.* **1996**, *271*, 8556.
(4) Liu, X. D.; Diao, H. Y.; Nishi, N. *Chem. Soc. Rev.* **2008**, *37*, 2745.
(5) Gartner, L. P.; Hiatt, J. L. *Color Textbook of Histology*, 2nd ed.; Saunders: Philadelphia, PA, 2001.
(6) Hartgerink, J. D.; Beniash, E.; Stupp, S. I. *Science* **2001**, *294*, 1684.
(7) Perumal, S.; Antipova, O.; Orgel, J. P. *Proc. Natl. Acad. Sci. U.S.A.* **2008**, *105*, 2824.
(8) Hirst, L. S.; Pynn, R.; Bruinsma, R. F.; Safinya, C. R. *J. Chem. Phys.* **2005**, *123*, 104902.
(9) Conwell, C. C.; Hud, N. V. *Biochemistry* **2004**, *43*, 5380.
(10) Rädler, J. O.; Koltover, I.; Salditt, T.; Safinya, C. R. *Science* **1997**, *275*, 810.
(11) Koltover, I.; Salditt, T.; Rädler, J. O.; Safinya, C. R. *Science* **1998**, *281*, 78.
(12) Bockstaller, M.; Köhler, W.; Wegner, G.; Fytas, G. *Macromolecules* **2001**, *34*, 6353.
(13) Bockstaller, M.; Köhler, W.; Wegner, G.; Vlassopoulos, D.; Fytas, G. *Macromolecules* **2001**, *34*, 6359.
(14) Kroeger, A.; Belack, J.; Larsen, A.; Fytas, G.; Wegner, G. *Macromolecules* **2006**, *39*, 7098.
(15) Kroeger, A.; Deimede, V.; Belack, J.; Lieberwirth, I.; Fytas, G.; Wegner, G. *Macromolecules* **2007**, *40*, 105.
(16) Viale, S.; best, A. S.; Mendes, E.; Jager, W. F.; Picken, S. J. *Chem. Commun.* **2004**, *14*, 1596.
(17) Viale, S.; Best, A. S.; Mendes, E.; Picken, S. J. *Chem. Commun.* **2005**, *12*, 1528.
(18) Viale, S.; Li, N.; Schotman, A. H.; Best, A. S.; Picken, S. J. *Macromolecules* **2005**, *38*, 3647.

(19) Every, H. A.; Van der Ham, L. V.; Picken, S. J.; Mendes, E. *Soft Matter* **2009**, *5*, 342.
(20) Funaki, T.; Kaneko, T.; Yamaoka, K.; Ohsedo, Y.; Gong, J. P.; Osada, Y.; Shibasaki, Y.; Ueda, M. *Langmuir* **2004**, *20*, 6518.
(21) Yang, W.; Furukawa, H.; Shigekura, Y.; Shikinaka, K.; Osada, Y.; Gong, J. P. *Macromolecules* **2008**, *41*, 1791.
(22) Shigekura, Y.; Chen, Y. M.; Furukawa, H.; Kaneko, T.; Kaneko, D.; Osada, Y.; Gong, J. P. *Adv. Mater.* **2005**, *17*, 2695.
(23) Shigekura, Y.; Furukawa, H.; Yang, W.; Chen, Y. M.; Kaneko, D.; Osada, Y.; Gong, J. P. *Macromolecules* **2007**, *40*, 2477.
(24) Wu, Z. L.; Furukawa, H.; Yang, W.; Gong, J. P. *Adv. Mater.* **2009**, *21*, 4696.
(25) Wu, Z. L.; Kurokawa, T.; Liang, S. M.; Gong, J. P. *Macromolecules* **2010**, *43*, 8202.
(26) Wu, Z. L.; Kurokawa, T.; Liang, S. M.; Furukawa, H.; Gong, J. P. *J. Am. Chem. Soc.* **2010**, *132*, 10064.
(27) Wu, Z. L.; Arifuzzaman, M.; Kurokawa, T.; Furukawa, H.; Gong, J. P. *Soft Matter* **2011**, *7*, 1884−1889.
(28) Arifuzzaman, M.; Wu, Z. L.; Kurokawa, T.; Kakugo, A.; Gong, J. P. *Soft Matter* **2012**, *8*, 8060.
(29) Yang, W.; Furukawa, H.; Gong, J. P. *Adv. Mater.* **2008**, *20*, 4499.
(30) Wu, Z. L.; Kurokawa, T.; Sawada, D.; Hu, J.; Furukawa, H.; Gong, J. P. *Macromolecules* **2011**, *44*, 3535−3541.
(31) Wu, Z. L.; Sawada, D.; Kurokawa, T.; Kakugo, A.; Yang, W.; Furukawa, H.; Gong, J. P. *Macromolecules* **2011**, *44*, 3542−3547.
(32) Wu, Z. L.; Gong, J. P. *NPG Asia Mater.* **2011**, *3*, 57.
(33) Pawlowski, W. P.; Gilbert, R. D.; Fornes, R. E.; Purrington, S. T. *J. Polym. Sci., Part B: Polym. Phys.* **1988**, *26*, 1101.
(34) Flory, P. J. *Proc. R. Soc. London, Ser. A* **1956**, *234*, 60.
(35) Flory, P. J. *Proc. R. Soc. London, Ser. A* **1956**, *234*, 73.
(36) Vandenberg, E. J.; Diveley, W. R.; Filar, L. J.; Pater, S. R.; Barth, H. G. *J. Polym. Sci., Part A: Polym. Chem.* **1989**, *27*, 3745.
(37) Sarkar, N.; Kershner, L. D. *J. Appl. Polym. Sci.* **1996**, *62*, 393.
(38) Demus, D.; Goodby, J.; Gray, G. W.; Spiess, H. W.; Vill, V. *Handbook of Liquid Crystal*; Wiley-VCH: Weinheim, Germany, 1998.
(39) Here C_P is the total concentration of the solution. Although after phase separation the upper and bottom phases have different PBDT concentration, we still use C_P for simplicity to note the integrated sample.
(40) Chen, W.; Sato, T.; Teramoto, A. *Macromolecules* **1998**, *31*, 6506.
(41) Ureña-Bebavides, E. E.; Ao, G.; Davis, V. A.; Kitchens, C. L. *Macromolecules* **2011**, *44*, 8990.
(42) Crawford, G. P.;Zumer, S. *Liquid Crystals in Complex Geometries*: Taylor &Francis: London, 1996.
(43) Haseloh, S.; van der Schoot, P.; Zentel, R. *Soft Matter* **2010**, *6*, 4112.
(44) Verhoeff, A. A.; Bakelaar, I. A.; Otten, R. H. J.; van der Schoot, P.; Lekkerkerker, H. N. W. *Langmuir* **2011**, *27*, 116.
(45) Wang, L.; Bloomfield, V. A. *Macromolecules* **1991**, *24*, 5791.
(46) Castelletto, V.; Itri, R.; Amaral, L. Q. *Macromolecules* **1995**, *28*, 8395.
(47) Skibinska, L.; Liu, H.; Patkowski, A.; Fischer, E. W.; Pecora, R. *J. Chem. Phys.* **1999**, *110*, 1794.
(48) Hirai, A.; Inui, O.; Horii, F.; Tsuji, M. *Langmuir* **2009**, *25*, 497.
(49) In our previous work (ref 21), dynamic light scattering (DLS) measurements revealed that the correlation length of PBDT assemblies increased with C_P approximately from several tens of nanometers to one micrometer, indicating the increase in bundle length. The isotropic cluster of long fibrils without long-range orientation was observed by TEM (Figure 5c). It should be reasonable to image the anisotropic fibrillar structures with long-range orientation existed in the nematic domains.
(50) Chandler, D. *Nature* **2005**, *437*, 640.
(51) Li, L. S.; Walda, J.; Manna, L.; Alivisatos, A. P. *Nano Lett.* **2002**, *2*, 557.
(52) Yuan, J.; Xu, Y.; Walther, A.; Bolisetty, S.; Schumacher, M.; Schmalz, H.; Ballauff, M.; Müller, A. H. E. *Nat. Mater.* **2008**, *7*, 718.
(53) The Maltese crosses in the POM images (Figure 6b−f) are not so perfect, because the PBDT molecules within the droplets could not align well when the droplets move energetically and the shearing field exists.